FINITE ELEMENT METHOD APPLIED TO THE QUENCHING OF STEEL CYLINDERS USING A MULTI-PHASE CONSTITUTIVE MODEL

Wendell Porto de Oliveira, wendell@furnas.com.br
Marcelo Amorim Savi, savi@mecanica.ufrj.br
UFRJ/COPPE – Department of Mechanical Engineering - 21.941.972 – Rio de Janeiro – RJ, P.O. Box 68.503 - Brazil

Pedro Manuel Calas Lopes Pacheco, calas@cefet-rj.br
CEFET/RJ – PPEMM - Department of Mechanical Engineering - 20.271.110 - Rio de Janeiro - RJ - Brazil

Abstract. Quenching is a commonly used heat treatment process employed to control the mechanical properties of steels. In brief, quenching consists of raising the temperature of the steel above a certain critical temperature, called austenitizing temperature, holding it at that temperature for a fixed time, and then rapidly cooling it in a suitable medium to room temperature. The resulting microstructures formed from quenching (pearlite, ferrite, bainite and martensite) depend on cooling rate and on steel characteristics. This article deals with the modeling and simulation of quenching in steel cylinders using a multi-phase constitutive model. The through hardening of a cylindrical body is considered as an application of the proposed general formulation. Finite element method is employed for spatial discretization. Numerical simulations present a good agreement with experimental data. Residual stress investigation is carried out analyzing the influence of the cooling medium during quenching process.

Keywords: Quenching, modeling, finite element method, residual stresses

1. INTRODUCTION

Quenching is a heat treatment usually employed in industrial processes. It provides a mean to control some mechanical properties of steels as tensile strength, toughness and hardness. The process consists of raising the steel temperature above a certain critical value, holding it at that temperature for a fixed time and then rapidly cooling it in a suitable medium to room temperature. The phases and constituents formed from quenching results in different microstructures (ferrite, cementite, pearlite, upper bainite, lower bainite and martensite) which depend on cooling rate and on chemical composition of the steel. The volume variation associated with phase transformation combined with large temperature gradients and non-uniform cooling can promote high residual stresses in quenched steels. As these internal stresses can produce warping and even cracking of a steel body, the prediction of such stresses is an important task (Sjöström, 1985; Denis *et al.*, 1985, 1999; Denis, 1996; Fernandes *et al.*, 1985; Woodard, *et al.*, 1999; Sen *et al.*, 2000; Çetinel *et al.*, 2000, Gür & Tekkaya, 2001). Nevertheless, the proposed models are not generic and are usually applicable to simple geometries.

Phenomenological aspects of quenching involve couplings among different physical processes and its description is unusually complex. Basically, three couplings are essential: thermal, phase transformation and mechanical phenomena. The description of each one of these phenomena has been addressed by several authors by considering these aspects separately. Sen *et al.* (2000) considered steel cylinders without phase transformations. There are also references that focus on the modeling of the phase transformation phenomenon (Hömberg, 1996; Chen *et al.*, 1997, Çetinel *et al.*, 2000; Reti *et al.*, 2001). Several authors have proposed coupled models that are not generic and are usually applicable to simple geometries as cylinders (Inoue & Wang, 1985; Melander, 1985; Sjöström, 1985; Denis *et al.*, 1985, 1987, 1999; Denis, 1996; Fernandes *et al.*, 1985; Woodard, *et al.*, 1999). Moreover, there are some complex aspects that are usually neglected in the analysis of quenching process. As an example, one could mention the heat generated during phase transformation. This phenomenon is usually treated by means of the latent heat associated with phase transformation (Inoue & Wang, 1985; Denis *et al.*, 1987, 1999; Woodward *et al.*, 1999). Meanwhile, other coupling terms in the energy equation related to other phenomena as plastic strain or hardening are not treated in literature and their analysis is an important topic to be investigated. Silva *et al.* (2004) analyzed the thermomechanical coupling during quenching considering austenite-martensite phase transformations. Silva *et al.* (2005) employed the finite element method to study the phase transformation effect in residual stresses generated by quenching in notched steel cylinders.

This article deals with the modeling and simulation of quenching in steel cylinders using a multi-phase constitutive model with internal variables formulated within the framework of continuum mechanics and the thermodynamics of irreversible processes. A numerical procedure is developed based on the operator split technique associated with an iterative numerical scheme in order to deal with nonlinearities in the formulation. With this assumption, the coupled governing equations are solved to obtain the temperature, stress and phase fields from four uncoupled problems: thermal, phase transformation, thermoelastic and elastoplastic. Classical numerical methods are applied to the uncoupled problems. The proposed general formulation is applied to the quenching of steel cylinders. An example

considering through hardening with two cooling mediums is presented. Numerical results present good agreement with those of experimental data obtained by the authors in previous works.

2. PHENOMENOLOGICAL ASPECTS OF PHASE TRANSFORMATIONS

In quenching process, a steel piece is heated and maintained at constant temperature until austenite is obtained. Afterwards, a cooling process promotes the transformation of austenite phase into different phases and constituents which results in microstructures as: ferrite, cementite, pearlite, upper bainite, lower bainite and martensite. It can be observed that the microstructure of carbon alloy steel, depending on its chemical composition, can be composed by phases (austenite, ferrite, cementite and martensite) and constituents (pearlite, upper bainite and lower bainite). In order to describe all these microstructures in a macroscopically point of view, the volume fraction of each one of the phases and constituents of these microstructures is represented by β_m (austenite $m = A$, ferrite $m = 1$, cementite $m = 2$, pearlite $m = 3$, upper bainite $m = 4$, lower bainite $m = 5$ and martensite $m = M$). All of these microstructural constituents and phases may coexist, satisfying the following constraints: $\beta_A + \beta_1 + \beta_2 + \beta_3 + \beta_4 + \beta_5 + \beta_M = 1$ and $0 \le \beta_m \le 1$.

Phase transformation from austenite to martensite is usually considered as a non-diffusive transformation, which means that amount of volume phase is only a function of temperature (Chen *et al.*, 1997; Çetinel *et al.*, 2000; Reti *et al.*, 2001). This process may be described by the equation proposed by Koistinen and Marburger (1959) and the evolution of martensitic phase can be written in a rate form as follows (Oliveira *et al.*, 2003, 2006; Oliveira, 2004, 2008):

$$\dot{\beta}_M\left(T,\dot{T}\right) = \varsigma_{A \to M}\, \beta_A^0 \left[\left(1 - \beta_M\right)\left(k\dot{T}\right)\right] \quad ; \quad \varsigma_{A \to M}\left(\dot{T},T\right) = \Gamma\left(-\dot{T}\right)\Gamma\left(M_s - T\right)\Gamma\left(T - M_f\right) \tag{1}$$

where β_A^0 is the amount of austenite at the beginning of transformation, k is a material property, T is the temperature and $\Gamma(x)$ is the Heaviside function. Under a stress-free state, M_s and M_f are the temperatures where martensitic transformation starts and finishes its formation.

Pearlite, cementite, ferrite and bainite formations are usually considered as diffusion-controlled transformation, which means that they are time dependent. The evolution of these phase transformations can be predicted through an approximate solution using data from Time-Temperature-Transformation diagrams (*TTT*) (Çetinel *et al.*, 2000; Reti *et al.*, 2001) and considering that the cooling process may be represented by a curve divided in a sequence of isothermal steps where the phase evolution is calculated considering isothermal transformation kinetics expressed by a *JMAK* law (Avrami, 1940; Cahn, 1956; Çetinel *et al.*, 2000; Reti *et al.*, 2001). The rate form of volume phase *i* can be written as follows (Oliveira *et al.*, 2003, 2006; Oliveira, 2004, 2008):

$$\dot{\beta}_m = \varsigma_{A \to phase\,(i)}\left\{ N_m (b_m)^{(1/N_m)}\left(\hat{\beta}_m^{\max} - \beta_m\right)\left[\ln\left(\frac{\hat{\beta}_m^{\max}}{\hat{\beta}_m^{\max} - \beta_m}\right)\right]^{\left(1 - \frac{1}{N_m}\right)}\right\} \quad (m = 1, ..., 5) \tag{2}$$

where N_m is the Avrami exponent and b_m is a parameter that characterizes the rate of nucleation and growth processes (Avrami, 1940; Reti *et al.*, 2001). $\hat{\beta}_m^{\max} = \beta_m^{\max}\left[\sum_{j=1; j \neq i}^{5}\beta_j - \beta_M\right]$ ($m = 1, ..., 5$) where $\beta_m^{\max}$ represents the maximum volume fraction for a phase m and $\varsigma_{A \to phase\,(i)}\left(\dot{T}, t\right) = \Gamma\left(-\dot{T}\right)\Gamma\left(t_i^f - t\right)\Gamma\left(t - t_m^s\right)$.

3. CONSTITUTIVE MODEL

Constitutive equations may be formulated within the framework of continuum mechanics and the thermodynamics of irreversible processes, by considering thermodynamic forces, defined from the Helmholtz free energy, ψ, and thermodynamic fluxes, defined from the pseudo-potential of dissipation, ϕ (Pacheco *et al.*, 2001).

The proposed phenomenological quenching model allows one to identify different aspects related to quenching process. With this aim, a Helmholtz free energy is proposed as a function of observable variables, total strain, ε_{ij}, and temperature, T. Moreover, the following internal variables are considered: plastic strain, ε_{ij}^p, volume fractions of seven different microstructures, represented by phases in a macroscopic point of view, $\beta = (\beta_0, \beta_1, \beta_2, \beta_3, \beta_4, \beta_5, \beta_6)$. A variable related to kinematic hardening, α_{ij}, is also considered. Therefore, the following free energy is proposed, employing indicial notation where summation convention is evoked, except when indicated (Oliveira *et al.*, 2003, 2006; Oliveira, 2004, 2008):

$$\rho\psi\big(\varepsilon_{ij}, \epsilon_{ij}^{p}, \alpha_{ij}, \epsilon_{ij}^{tv}, \epsilon_{ij}^{tp}, T, \beta_0, \beta_1, \beta_2, \beta_3, \beta_4, \beta_5, \beta_6\big) = W\big(\varepsilon_{ij}, \epsilon_{ij}^{p}, \alpha_{ij}, \epsilon_{ij}^{tv}, \epsilon_{ij}^{tp}, T, \beta_0, \beta_1, \beta_2, \beta_3, \beta_4, \beta_5, \beta_6\big) =$$
$$= \sum_{m=0}^{6} \beta_m W^{(m)}\big(\varepsilon_{ij}, \epsilon_{ij}^{p}, \alpha_{ij}, \epsilon_{ij}^{tv}, \epsilon_{ij}^{tp}, T\big) + W_{\beta}\big(\beta_0, \beta_1, \beta_2, \beta_3, \beta_4, \beta_5, \beta_6\big) \tag{3}$$

where ρ is the material density and $W_{\beta}(\beta_0, \beta_1, \beta_2, \beta_3, \beta_4, \beta_5, \beta_6) = J_{\pi}(\beta_0, \beta_1, \beta_2, \beta_3, \beta_4, \beta_5, \beta_6)$ represents the indicator function associated with the convex π.

$$\pi = \{\beta_m \in \Re \mid 0 \le \beta_m \le 1 \ (m = 0, 1, \dots, 6); \sum_{m=0}^{6} \beta_m = 1 \ \} \tag{4}$$

The elastic strain can be written assuming an additive decomposition: $d\varepsilon_{ij}^{e} = d\varepsilon_{ij} - d\varepsilon_{ij}^{p} - \left(\sum_{m=0}^{6} \beta_m \alpha_T^{(m)}\right) dT\delta_{ij} - d\varepsilon_{ij}^{tv} - d\varepsilon_{ij}^{tp}$. In the right hand side of this expression, the first term is the total strain while the second is related to plastic strain. The third term is associated with thermal expansion. The parameter $\alpha_T^{(m)}$ is the coefficient of linear thermal expansion associated to phase m and δ_{ij} is the Kronecker delta. The fourth term is related to volumetric expansion associated with phase transformation from a parent phase $d\varepsilon_{ij}^{tv} = (\sum_{m=1}^{6} \gamma_m d\beta_m)\delta_{ij}$, where γ_m is a material phase property related to total expansion. Finally, the last term is denoted as transformation plasticity strain $d\varepsilon_{ij}^{tp} = \sum_{m=1}^{6} \frac{3}{2}\kappa_m f'(\beta_m)d\beta_m \sigma_{ij}^{d}$, being the result of several physical mechanisms related to local plastic strain promoted by the phase transformation (Denis *et al.*, 1985; Sjöström, 1985); κ_m is a material phase parameter, $f(\beta_m)$ expresses the transformation process dependence and σ_{ij}^{d} the deviatoric stress defined by $\sigma_{ij}^{d} = \sigma_{ij} - \delta_{ij}(\sigma_{kk}/3)$, with σ_{ij} being the stress tensor component. It should be emphasized that this strain may be related to stress states that are inside the yield surface.

In order to describe dissipation processes, it is necessary to introduce a potential of dissipation or its dual, which can be split into two parts $\phi^*(P_{ij}, Q_{ij}, R_{ij}, X_{ij}, B^{\beta}, g_i) = \phi_I^*(P_{ij}, Q_{ij}, R_{ij}, X_{ij}, B^{\beta}) + \phi_T^*(g_i)$ The set of constitutive equations is composed by the thermodynamics forces (σ_{ij}, P_{ij}, Q_{ij}, R_{ij}, X_{ij}, T, B^{β}, g_i), associated with state variables ($\epsilon_{ij}, \epsilon_{ij}^{p}, \epsilon_{ij}^{tv}, \epsilon_{ij}^{tp}, \alpha_{ij}, s, \beta$), and the thermodynamic fluxes are defined as follows:

$$\sigma_{ij} = \frac{\partial W}{\partial \varepsilon_{ij}} = \sum_{m=0}^{6} \beta_m E_{ijkl}^{(m)}\big[\varepsilon_{kl} - \varepsilon_{kl}^{p} - \alpha_T^{(m)}(T - T_0)\delta_{kl} - \varepsilon_{kl}^{tv} - \varepsilon_{kl}^{tp}\big] \tag{5}$$

$$P_{ij} = -\frac{\partial W}{\partial \varepsilon_{ij}^{p}} = \sigma_{ij} \quad ; \quad Q_{ij} = -\frac{\partial W}{\partial \varepsilon_{ij}^{tv}} = \sigma_{ij} \quad ; \quad R_{ij} = -\frac{\partial W}{\partial \varepsilon_{ij}^{tp}} = \sigma_{ij} \quad ; \quad X_{ij} = -\frac{\partial W}{\partial \alpha_{ij}} = \big[\sum_{m=0}^{6} \beta_m H_{ijkl}^{(m)}\big]\alpha_{kl} \tag{6}$$

$$s = -\frac{1}{\rho}\frac{\partial W}{\partial T} \quad ; \quad B^{\beta_m} = -\frac{\partial W}{\partial \beta_m} \in -\partial_{\beta_m} J_{\pi} - \Big[\frac{\partial W_e}{\partial \beta_m} + \frac{\partial W_\alpha}{\partial \beta_m} + \frac{\partial W_T}{\partial \beta_m}\Big] \ (m = 1, \dots, 6) \tag{7}$$

$$\dot\varepsilon_{ij}^{p} \in \partial_{P_{ij}} I_m^*(P_{ij}, X_{ij}) = \lambda \, sign\big[\sigma_{ij} - (\sum_{m=0}^{6} \beta_r H_{ijkl}^{(m)})\alpha_{kl}\big] \quad ; \quad \dot\alpha_{IJ} \in -\partial_{X_{ij}} I_m^*(\sigma_{ij}, X_{ij}) = \dot\varepsilon_{ij}^{p} \tag{8}$$

$$\dot\varepsilon_{ij}^{tv} = \frac{\partial \phi^*}{\partial Q_{ij}} = \sum_{r=1}^{6} \gamma^{(r)} \dot\beta_r \delta_{ij} \ ; \ \dot\varepsilon_{ij}^{tp} = \frac{\partial \phi^*}{\partial R_{ij}} = \sum_{m=1}^{6} \frac{3}{2}\kappa^{(m)} f'(\beta_m) \dot\beta_m \sigma_{ij}^{d} \ ; \tag{9}$$

$$\dot\beta_M = \frac{\partial \phi^*}{\partial B^{\beta_M}} = \zeta_{A \to M}\beta_A^0\big[(1 - \beta_M)k\dot T\big] \tag{10}$$

$$\dot\beta_m = \frac{\partial \phi^*}{\partial B^{\beta_m}} = \zeta_{A \to m}\left\{N_m(b_m)^{\left(\frac{1}{N_m}\right)}(\hat\beta_m^{max} - \beta_m)\Big[ln\Big(\frac{\hat\beta_m^{max}}{\hat\beta_m^{max} - \beta_m}\Big)\Big]^{\left(1 - \frac{1}{N_m}\right)}\right\} \ (m = 1, \dots, 5) \tag{11}$$

$$q_i = -\frac{\partial \phi^*}{\partial g_i} = -\big[\sum_{m=0}^{6} \beta_m \Lambda^{(m)}\big]Tg_i = -\big[\sum_{m=0}^{6} \beta_m \Lambda^{(m)}\big]\frac{\partial T}{\partial x_i} \tag{12}$$

where $\partial_{\beta_r} J_{\pi}$ is the sub-differential of the indicator function J_{π}, $I_m^*(P_{ij}, X_{ij})$ is the indicator function associated with elastic domain, related to the *von Mises* criterion, λ is the plastic multiplier from the classical theory of plasticity (Lemaitre & Chaboche, 1990), sign(x) = x / |x| and q_i is the heat flux vector. By assuming that the specific heat is

$\left[\sum_{m=0}^{6} \beta_m c^{(m)}\right] = -\left(\frac{T}{\rho}\right) \partial^2 W / \partial T^2$ and the set of constitutive equations (5-12), the energy equation can be written as (Pacheco, 1994):

$$\frac{\partial}{\partial x_i}\left(\left[\sum_{m=0}^{6} \beta_r \Lambda^{(m)}\right] \frac{\partial T}{\partial x_i}\right) - \rho\left[\sum_{m=0}^{6} \beta_m c^{(m)}\right]\dot{T} = -a_I - a_T \qquad (13)$$

where:

$$\begin{cases} a_I = \sum_{m=1}^{6} B^{\beta_m} \dot{\beta}_m - X_{ij}\dot{\varepsilon}_{ij}^p + \sigma_{ij}(\dot{\varepsilon}_{ij}^p + \dot{\varepsilon}_{ij}^{tv} + \dot{\varepsilon}_{ij}^{tp}) \\ a_T = T\left[\frac{\partial \sigma_{ij}}{\partial T}(\dot{\varepsilon}_{ij} - \dot{\varepsilon}_{ij}^p - \dot{\varepsilon}_{ij}^{tv} - \dot{\varepsilon}_{ij}^{tp}) - \sum_{m=1}^{6} \frac{\partial B^{\beta_m}}{\partial T}\dot{\beta}_m + \frac{\partial X_{ij}}{\partial T}\dot{\varepsilon}_{ij}^p\right] \end{cases} \qquad (14)$$

Terms a_I and a_T are, respectively, internal and thermal coupling. The thermomechanical coupling effect related to phase transformation may be represented as a latent heat released during the phase transformation (Fernandes *et al.*, 1985; Denis *et al.*, 1987; Woodard *et al.*, 1999): $a_I + a_T = \dot{Q} = \sum_{m=1}^{6} \Delta H_m \dot{\beta}_m$ where ΔH_m is the enthalpy variation in a transformation process involving a previous phase (austenite) and a product phase β_m (m = 1, ..,6). Therefore, this source term is used instead of all thermomechanical couplings effects, which represents a first approach of the general formulation (Silva *et al.*, 2004).

4. CYLINDRICAL BODIES

This contribution considers cylindrical bodies as an application of the proposed general formulation. An axisymmetric finite element model is developed to study the quenching process in cylinders. The numerical procedure here proposed is based on the operator split technique (Ortiz *et al.*, 1983; Pacheco, 1994) associated with an iterative numerical scheme in order to deal with nonlinearities in the formulation. With this assumption, coupled governing equations are solved from four uncoupled problems: thermal, phase transformation, thermo-elastic and elastoplastic.

Thermal Problem - Comprises a conduction problem with convection and radiation. Material properties depend on temperature, and therefore, the problem is governed by non-linear parabolic equations. Finite element method is used for numerical solution.

Phase Transformation Problem – The volume fractions of the phases are determined in this problem. Evolution equations are integrated from a simple implicit Euler method.

Thermo-elastic Problem - Stress and displacement fields are evaluated from temperature distribution. Numerical solution is obtained employing the finite element method.

Elastoplastic Problem - Stress and strain fields are determined considering the plastic strain evolution in the process. Numerical solution is based on the classical return mapping algorithm (Simo & Hughes, 1998).

A detailed description of the model could be found in Pacheco *et al.* (2001), Silva *et al.* (2004, 2005) and Oliveira (2008).

5. EXPERIMENTAL PROCEDURE

The experimental procedure adopted consists of heating cylindrical specimens with external radius R = 25.4 mm = 1", made by SAE 4140H, in a furnace to a suitable austenitizing temperature (830°C), holding at that temperature for a sufficient time to promote the desired change in crystalline structure in all parts of the workpiece (1 hour), and finally cooling in two different media: air and water. Four cylindrical specimens are used: one specimen with two holes (one at the cylinder center and the other at 1 mm from the cylinder surface) and three other specimens with one hole at the cylinder center. Thermocouples are introduced at each hole and the temperature time history is acquired and registered by a data acquisition system. Figure 1 shows the furnace, the data acquisition system and the cylindrical specimen (Oliveira *et al.*, 2003; Oliveira, 2004).
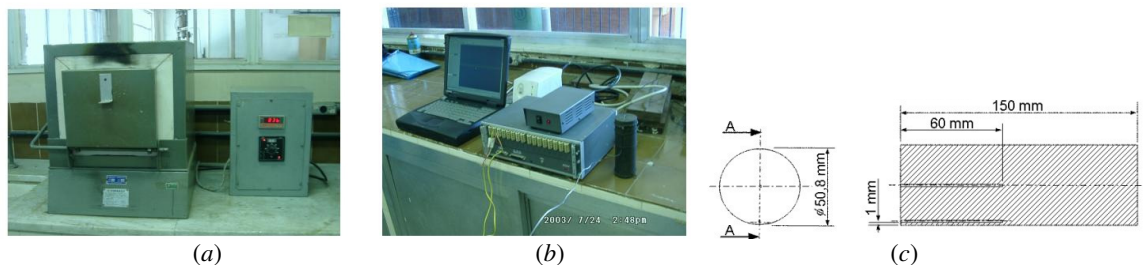

(a)   *(b)*   *(c)*

Figure 1. (*a*) Furnace, (*b*) data acquisition system and (c) cylindrical specimen.

5.1. Air Cooling

At first, air cooling medium is of concern. Figure 2 presents the temperature time history curves. Figure 2*a* presents the thermocouple response at the center of the specimen and also at 1 mm from the cylinder surface. On the other hand, Fig. 2*b* shows the response from different specimens where the thermocouple is at the cylinder center. It should be pointed out that, when the specimen is about 650°C, a temperature increase can be observed. This phenomenon is related to the thermomechanical coupling (Silva *et al.*, 2004; Denis, 1996; Woodard *et al.*, 1999) associated with the latent heat of the austenite → pearlite phase transformation.

(*a*)   (*b*)
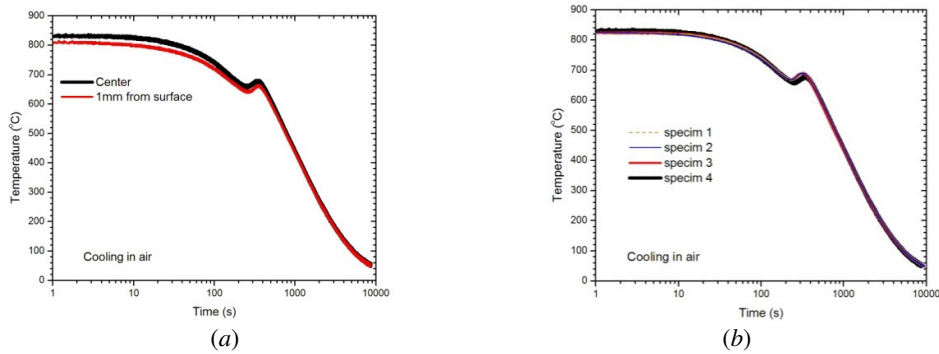
Figure 2. (*a*) Air cooling temperature evolution at the center and at 1 mm from the cylinder surface. (*b*) Temperature time history from four specimens measured at the cylinder center.

Figure 3 presents the microstructure at an internal cross section of the cylinder far from the edges, at three regions (*r* = 0, *r* = 0.5 *R* and *r* = *R*). The metallographic analysis developed reveals a homogeneous radial phase distribution with 24% of ferrite and 76% of pearlite.
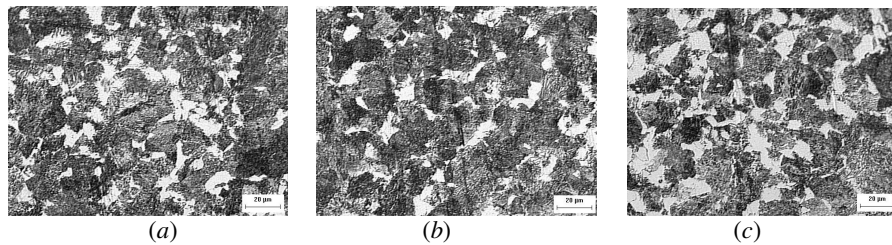

(*a*)   (*b*)   (*c*)

Figure 3. Air cooling specimen microstructure: (*a*) center (*r* = 0), (*b*) *r* = 0.50*R* and (*c*) surface (*r* = *R*).

5.2. Water Cooling

At this point, water cooling medium is considered. This is related to severe quenching conditions and it is expected a great level of matensitic formation. Figure 4 presents the temperature time history curves while Fig. 5 presents the metallographic analysis. The metallographic analysis developed reveals a homogeneous radial phase distribution with 100% of martensite after the quenching process.
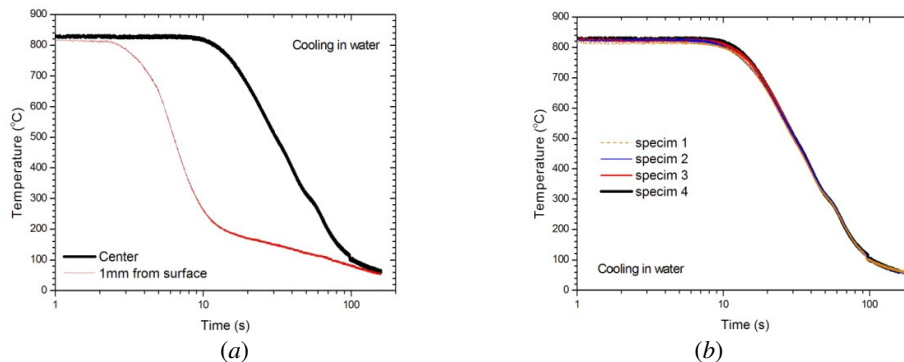

(*a*)   (*b*)

Figure 4. (*a*) Temperature time history at the center and at 1 mm from the surface for the cylinders. (*b*) Temperature time history for four specimens cooled in water.
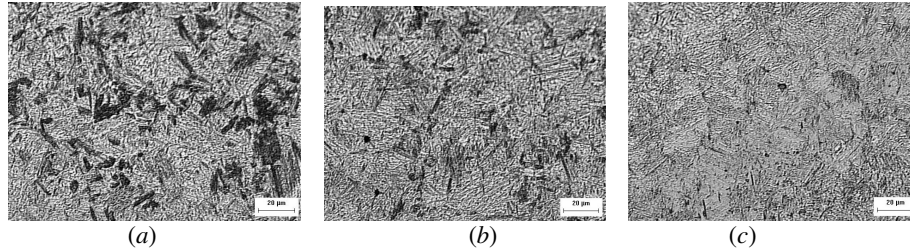
(a)   (b)   (c)

Figure 5. Water cooling specimen microstructure: (a) center ($r = 0$), (b) $r = 0.50R$ and (c) suface ($r = R$).

6. NUMERICAL RESULTS

The forthcoming analysis tries to reproduce the conditions of the experiment described in the last section using numerical simulations related to the developed model for the two quenching processes discussed: air and water cooling. Therefore, a SAE 4140H, 25.4mm (1") radius cylinder quenched in air and water are considered.

Material parameters of the SAE 4140H are the following (Denis $et\ al.$, 1985, 1999; Woodard, $et\ al.$, 1999; Sjöström, 1985; Melander, 1985; Oliveira, 2004): $\gamma_1 = 3.333 \times 10^{-3}$, $\gamma_2 = 0$, $\gamma_3 = \gamma_4 = \gamma_5 = 5.000 \times 10^{-3}$, $\gamma_6 = 1.110 \times 10^{-2}$, $\kappa_m = \left[5/\left(2\sigma_Y^o\right)\right]\gamma_m$ (where σ_Y^o is the austenite yielding stress and $m = 1,...,6$), $\rho = 7.800 \times 10^3\ kg/m^3$, $M_s = 340°C$, $M_f = 140°C$. Other parameters depend on temperature and needs to be interpolated from experimental data. Therefore, parameters $E^m, H^m, \sigma_Y^m, \alpha_T^m, c^m, \Lambda^m$ ($m = 1,...,6$) and the convection coefficient, h, are evaluated by polynomial expressions (Melander, 1985; Hildenwall, 1979; Pacheco $et\ al.$, 2001; Silva $et\ al.$, 2004). Temperature dependent parameters for diffusive phase transformations are obtained from TTT diagrams (ASM, 1977). Moreover, latent heat released associated with the enthalpy variation in a transformation process involving a parent phase (austenite) and a product phase β_m are given by: $\Delta H_1 = 1.55 \times 10^9 - 2.31 \times 10^6 T + 1597 T^2 - 0.429 T^3 - 5.00 \times 10^{11}/T$ J/m^3, $\Delta H_3 = \Delta H_4 = \Delta H_5 = 1.56 \times 10^9 - 1.5 \times 10^6 T\ \ J/m^3$, $\Delta H_6 = 640 \times 10^6\ \ J/m^3$ (Denis $et\ al.$, 1987; Woodard $et\ al.$, 1999; Stull & Prophet, 1971).

Finite element analysis is performed exploiting a single strip axisymmetrical geometry for simulations. For long cylinders subjected to through hardening, far from the ends, the process along the cylinder is similar and the analysis can be performed in a thin strip. Figure 6 shows the axisymmetric finite element model mesh obtained after a convergence analysis where z is axissymmetry axis. Mechanical and thermal boundary conditions are associated with plane stress condition: prescribed z-direction null displacement at $z = 0$ (symmetry condition); prescribed z-direction null heat flux at $z = 0$ and $z = h$; and convection and radiation at external surface. In all simulations developed τ_{rz} present small values in the whole piece.
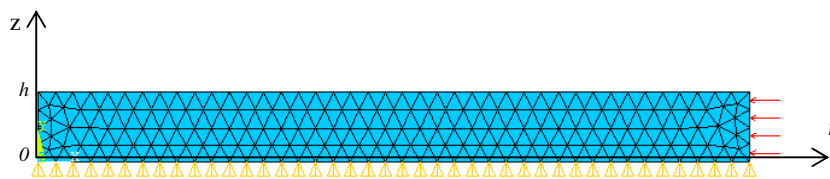

Figure 6. Finite element mesh and boundary conditions.

6.1. Air Cooling

In order to compare numerical and experimental results, it is presented in Fig. 7 the temperature time history in two different positions: at the center and at 1 mm from the surface of the cylinder. It is noticeable the close agreement between results and it is important to highlight that the thermomechanical coupling effect is captured by the model. As expected, the model shows the temperature increase at about 650°C, which is associated with the latent heat of the austenite → pearlite phase transformation. In terms of volume fraction distribution, model predicts 27% of ferrite and 73% of pearlite that is in close agreement with experimental results.

The behavior of the stress field during the quenching process is now in focus. Figure 8 presents the stress evolution (σ_r, σ_θ and σ_z) for five different positions: $r = 0$; $r = 1/4R$; $r=1/2R$; $r = 3/4R$; $r=R$.
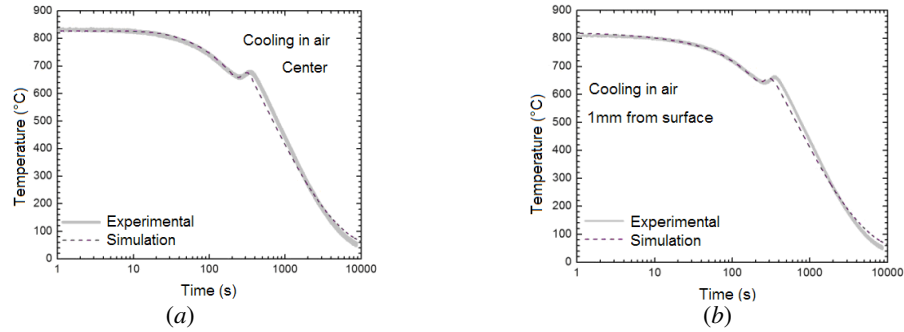
Figure 7. Air cooling temperature time history: (*a*) at the center and (*b*) at 1 mm from the cylinder surface.
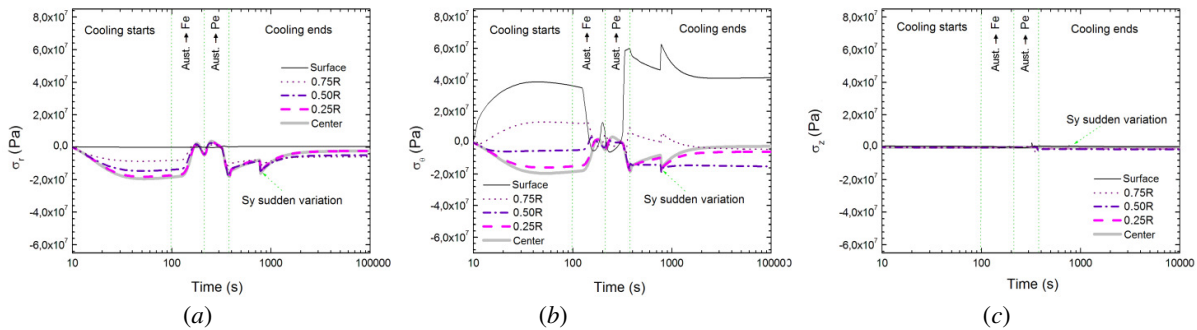

Figure 8. Stress distribution during the time: (*a*) σ_r, (*b*) σ_θ and (*c*) σ_z.

Basically, the stress time evolution can be understood due to the main phenomena observed: start cooling, phase transformation and end cooling. Component τ_{rz} has low values during all the process and, therefore, will be neglected in the analysis. A description of stress evolution, along each these steps, is now presented.

Before the cooling starts, σ_r and σ_θ stress components are close to zero in the whole piece. Component σ_z also presents values close to zero. When the cooling process starts, the cylinder temperature is at austenitization region and phase transformation is not involved. The σ_r stress component is always null at $r = R$ because the absence of mechanical boundary conditions at cylinder surface.

Convection and radiation phenomena induce faster cooling at the cylinder surface promoting a contraction of this region in contrast of the expansion at the center of the cylinder. Therefore, it is observed the stress distribution behavior summarized below:

- σ_r - Compressive behavior at cylinder center that tends to be close to zero near the surface;
- σ_θ - Tensile behavior at the cylinder surface and compressive at the center;
- σ_z - This stress component tends to be close to zero in the whole piece;

The phase transformation process has an important influence in stress distribution during quenching process. There is a competition between phase transformation effects and thermal effects. At the beginning of the phase transformation, these effects are more important but, at the end of these transformations, the thermal effects become more relevant. In general, the following aspects can be understood:

- σ_r - Tensile behavior at the beginning and compressive behavior at the end of the phase transformation, at almost the whole piece, except close to the cylinder surface;
- σ_θ - At the beginning the cylinder presents compressive behavior at surface and tensile behavior at the center; at the end of the process there are tensile components at the surface and compressive values at the center;
- σ_z - Presents values close to zero;

The transformation from austenite to pearlite generates high values of stress levels when compared to austenite to ferrite transformation. This effect is due to the large amount of transformed volume fraction associated with pearlite. It is important to remember that part of residual stresses is absorbed by transformation plasticity.

After the phase transformation stage, temperatures at the cylinder surface are smaller than the temperatures at the center of the specimen. For temperatures above 475°C, the yield stress has low values and therefore, part of residual stresses is vanished. The stress behavior in this stage can be summarized as follows:

- σ_r - Compressive behavior at the center of the cylinder being zero close to the surface;
- σ_θ - Tensile behavior at the cylinder surface and compressive at the center;

- σ_z - Values tend to be close to zero in the whole piece;

6.2. Water Cooling

The quenching process in water is now in focus. Temperature time history in two different positions (at the center of the cylinder and at 1 mm from the cylinder surface) is presented in Fig. 9. At the body center there is a close agreement between numerical and experimental results. By considering the position at 1mm from the surface, on the other hand, results capture just the general behavior. This discrepancy is explained by the thermocouple influence. Actually, it is possible to make adjustments considering the heat conduction through the thermocouple and evaluating the temperature at its center. In terms of volume fraction distribution the model predicts 100% of martensite at the surface and 87% at the center of the cylinder. This implies an amount of 13% of bainite that is a small difference when compared to experimental data. Nevertheless, it is important to observe that experimental data uses optical analysis in order to conclude the phase distribution and therefore, this difference may be less than presented.
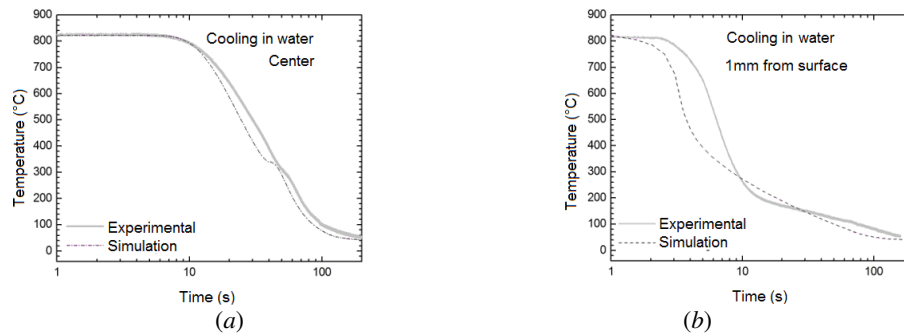

Figure 9. Air cooling temperature time history: (a) at the center and (b) at 1 mm from the surface for the cylinders.

Stress analysis is now in focus. Figure 10 present the stress time evolution (σ_r, σ_θ and σ_r) for five different positions: $r = 0$; $r = 1/4R$; $r=1/2R$; $r = 3/4R$; $r=R$.
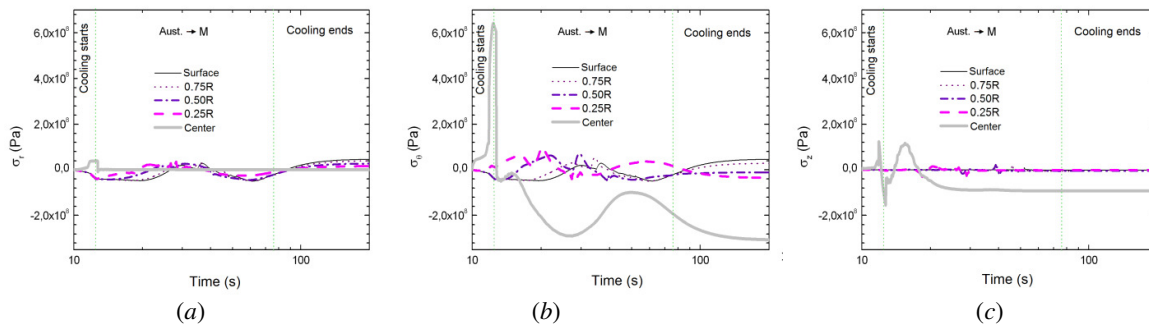

Figure 10. Stress distribution during the time, at plane stress: (a) σ_r, (b) σ_θ and (c) σ_z.

As previously discussed, the stress evolution can be understood from the main phenomena involved in the process: start cooling, phase transformation and end cooling. Before the cooling starts, σ_r and σ_θ have values close to zero in the whole piece. Component σ_z also presents values close to zero. In the same way of the air cooling description, the σ_r stress component is always null at $r = R$ due to the absence of mechanical boundary conditions at cylinder surface.

Convection and radiation phenomena induce faster cooling at the cylinder surface promoting a contraction of this region in contrast of the expansion at the center of the cylinder. Therefore, it is observed the stress distribution behavior discussed below:

- σ_r - Compressive behavior at the center of the cylinder, being close to zero at the surface;
- σ_θ - Tensile behavior at the cylinder surface and compressive at the center;
- σ_z - Tensile behavior at the cylinder surface and stress values tend to zero at other regions;

The phase transformations of this process can be associated with the transformation from austenite to upper bainite, to lower bainite and to martensite. Nevertheless, the martensitic transformation is the most important. The volumetric expansion due to phase transformation competes with high gradients of temperature and high cooling rates. At the beginning of the process, martensitic transformation effects are more important and, after that, the thermal effects became more relevant as the transformation rate rises. Under this condition, the following analysis can be done:

- σ_r - At the beginning of this stage, the value of this stress increases, being tensile at the center of the cylinder and zero at the surface; after that, the value of this stress decreases, being compressive at center of the cylinder and zero at the surface;
- σ_θ - This stress value decreases, becoming compressive; after that, this stress value increases in the whole piece being compressive;
- σ_z - This stress value initially increases at the cylinder surface, assuming tensile values and, after that, this stress value decreases, assuming compressive values; in all other regions of the cylinder, this stress tend to zero;

6.3. Residual Stresses

The use of water as a cooling medium makes quenching a severe process to the specimen. Under this condition, the mechanical behavior observed at the cylinder surface is more intense than other regions of the cylinder. Transformation plasticity plays an important role in this process changing the residual stress distribution. Figure 11 shows the residual stress distribution for the air and water cooling media at the end of the quenching process. At the end of the process, temperatures tend to be homogeneous in the whole piece and it is possible to identify permanent strains in the specimen. Water cooling presents large values when compared with air cooling.
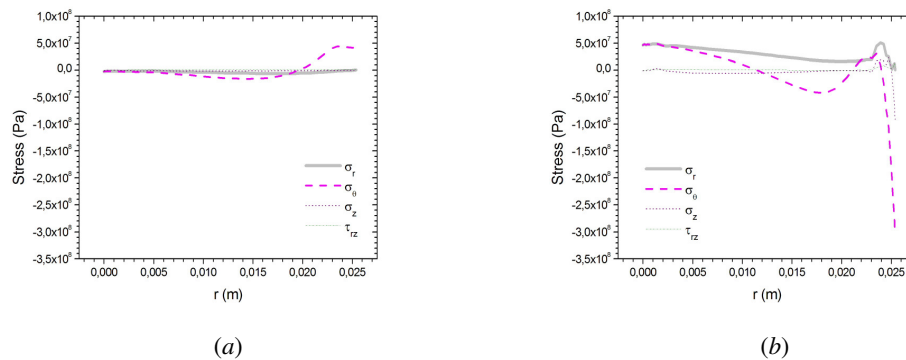

(a)   (b)

Figure 11. Stress distribution at the end of the process: (*a*) air and (*b*) water cooling.

7. CONCLUSIONS

This contribution deals with modeling and simulation of quenching process, presenting an anisothermal multi-phase constitutive model formulated within the framework of continuum mechanics and thermodynamics of irreversible processes. This approach allows a direct extension to more complex situations, as the analysis of three-dimensional media. A numerical procedure is developed based on the operator split technique associated with an iterative numerical scheme in order to deal with nonlinearities in the formulation. The proposed numerical procedure allows the use of traditional numerical methods, like the finite element method. Through hardening of cylindrical bodies is considered as application of the proposed general formulation. Numerical results show that the proposed model is capable of capturing the general behavior of experimental data. Therefore, it can be used as a tool to predict the thermomechanical behavior of quenched mechanical components and choose important parameters as the cooling medium and the induced layer thickness.

8. ACKNOWLEDGEMENTS

9. REFERENCES

ASM, 1977, *"Atlas of Isothermal Transformation and Cooling Transformation Diagrams"*, American Society Metals.
Avrami, M., 1940, "Kinetics of Phase Change. II: Transformation-Time relations for random distribution of nuclei", *Journal of Chem. Phys.*, v.8, pp.212.
Cahn, J. W., 1956, "Transformation Kinetics During Continuous Cooling", *Acta Metallurgica*, v.4, pp.572-575.
Çetinel, H., Toparlı, M. & Özsoyller, 2000, "A Finite Element Based Prediction of the Microstructural Evolution of Steels Subjected to the Tempcore Process", *Mechanics of Materials*, v.32, pp.339-347.
Chen, J. R., Tao, Y. Q. & Wang, H.G., 1997, "A Study on Heat Conduction with Variable Phase Transformation Composition during Quench Hardening", *Journal of Materials Processing Technology*, v.63, pp.554-558.

Denis, S., 1996, "Considering Stress-Phase Transformation Interaction in the Calculation of Heat Treatment Residual Stresses", *Journal de Physique IV*, v.6, January, pp.159-174.

Denis, S., Gautier, E., Simon, A. & Beck, G., 1985, "Stress-Phase-Transformation Interactions – Basic Principles, Modelling and Calculation of Internal Stresses", *Material Science and Technology*, v.1, October, p.805-814.

Denis, S., Sjöström, S. & Simon, A., 1987, "Coupled Temperature, Stress, Phase Transformation Calculation Model Numerical Illustration of the Internal Stresses Evolution during Cooling of a Eutectoid Carbon Steel Cylinder", *Metallurgical Transactions A*, v.18A, July, pp.1203-1212.

Denis, S., Archambault, S., Aubry, C., Mey, A., Louin, J. C. & Simon, A., 1999, "Modelling of Phase Transformation Kinetics in Steels and Coupling with Heat Treatment Residual Stress Predictions", *Journal de Physique IV*, v.9, September, pp.323-332.

Fernandes, M.B., Denis, S. & Simon, A., 1985, "Mathematical Model Coupling Phase Transformation and Temperature Evolution during Quenching of Steels", Materials Science and Technology, v.1, October, pp.838-844.

Gür, C.H. & Tekkaya, A.E., 2001, "Numerical Investigation of Non-Homogeneous Plastic Deformation in Quenching Process", *Materials Science and Engineering*, A319-321, pp.164-169.

Hildenwall, B., 1979, "*Prediction of the Residual Stresses Created During Quenching*", Ph.D. Thesis, Linkoping Univ.

Hömberg, D., 1996, "A Numerical Simulation of the Jominy End-quench Test", *Acta Mater.*, v.44, n.11, pp.4375-4385

Inoue, T. & Wang, Z., 1985, "Coupling between Stress, Temperature, and Metallic Structures during Processes Involving Phase Transformations", *Material Science and Technology*, v.1, pp.845-850.

Koistinen, D. P. & Marburger, R. E., 1959, "A General Equation Prescribing the Extent of the Austenite-Martensite Transformation In Pure Iron-Carbon Alloys and Plain Carbon Steels", *Acta Metallurgica*, v.7, pp.59-60.

Lemaitre, J. & Chaboche, J.L., 1990, *"Mechanics of Solid Materials"*, Cambridge Press Univ.

Melander, M., 1985, "*A Computational and Experimental Investigation of Induction and Laser Hardening*", Ph.D. Thesis, Department of Mechanical Eng., Linkoping University.

Ortiz, M., Pinsky, P. M. & Taylor, R. L., 1983, "Operator Split Methods for the Numerical Solution of the Elastoplastic Dynamic Problem", *Computer Methods in Applied Mechanics and Engineering*, v.39, pp.137-157.

Oliveira, W. P., Souza, L. F. G., Pacheco, P. M. C. L. & Savi, M. A., 2003, "Quenching Process Modeling in Steel Cylinders Using a Multi-Phase Constitutive Model", *COBEM 2003 - 17th International Congress of Mechanical Engineering*, São Paulo.

Oliveira, W. P., 2004, *"Modeling Quenching Process in Steel Cylinder Using Multi-Phase Constitutive Model"*, M.Sc. Dissertation, CEFET/RJ, in Portuguese.

Oliveira, W. P., 2008, *"Modeling and Simulation of Quenching in Axisimmetrical Geometries Using a Multi-Phase Constitutive Model"*, Ph.D. Thesis, COPPE/UFRJ, in Portuguese.

Oliveira, W.P., Savi, M.A., Pacheco, P.M.C.L. & de Souza, L.F.G, 2006; "Finite Element Analysis of the Thermomechanical Coupling in Quenching of Steel Cylinders Using a Constitutive Model with Diffusional Phase Transformations", *ECCM-2006 - III European Conference on Computational Mechanics*, Lisboa – Portugal.

Pacheco, P. M. C. L., 1994, *"Analysis of Thermomechanical Coupling in Elasto-viscous-plastic Materials"*, Ph.D. Thesis, Department of Mechanical Engineering, PUC-Rio.

Pacheco, P. M. C. L., Savi, M. A. & Camarão, A. F., 2001, "Analysis of Residual Stresses Generated by Progressive Induction Hardening of Steel Cylinders", *Journal of Strain Analysis for Engineering Design*, v.36, n.5, pp.507-516.

Reti, T., Fried, Z. & Felde, I., 2001, "Computer Simulation of Steel Quenching Process using a Multi-Phase Transformation Model", *Computational Materials Science*, v.22, pp.261-278.

Sen, S., Aksakal, B. & Ozel, A., 2000, "Transient and Residual Thermal Stresses in Quenched Cylindrical Bodies", *International Journal of Mechanical Sciences*, v.42 n.10, p.2013-2029.

Silva, E. P., Pacheco, P. M. C. L. & Savi, M. A., 2004, "On the Thermo-Mechanical Coupling in Austenite-Martensite Phase Transformation Related to the Quenching Process", *Int. J. of Solids and Struct.*, v.41, n.3-4, pp.1139-1155.

Silva, E. P., Pacheco, P. M. C. L. & Savi, M. A., 2005, "Finite Element Analysis of the Phase Transformation Effect in Residual Stresses Generated by Quenching in Notched Steel Cylinders", *Journal of Strain Analysis for Engineering Design*, v.40, n.2, p.151-160.

Simo, J. C. & Hughes, T. J. R., 1998, "*Computational Inelasticity*", Springer.

Sjöström, S., 1985, "Interactions and Constitutive Models for Calculating Quench Stresses in Steel", *Material Science and Technology*, v.1, p.823-829.

Stull, D. R. & Prophet, H., 1971, "*Janaf Thermochemical Tables*", National Standard Ref. Data System, 2 Ed. NBS 37.

Woodard, P. R., Chandrasekar, S. & Yang, H. T. Y., 1999, "Analysis of Temperature and Microstructure in the Quenching of Steel Cylinders", *Metallurgical and Materials Trans.*

10. RESPONSIBILITY NOTICE

The authors are the only responsible for the printed material included in this paper.